
A NON-ALTERNATING GRAPH HASHING ALGORITHM FOR LARGE SCALE IMAGE SEARCH

Sobhan Hemati

Kimia Lab
University of Waterloo
ON, Canada

Mohammad Hadi Mehdizavareh

School of Electrical and Computer Engineering
University of Tehran
Tehran, Iran

Shojaeddin Chenouri

Department of Statistics and Actuarial Science
University of Waterloo
ON, Canada

Hamid R Tizhoosh *

Kimia Lab and Vector Institute, MaRS Center
University of Waterloo
ON, Canada
tizhoosh@uwaterloo.ca

June 6, 2022

ABSTRACT

In the era of big data, methods for improving memory and computational efficiency have become crucial for successful deployment of technologies. Hashing is one of the most effective approaches to deal with computational limitations that come with big data. One natural way for formulating this problem is spectral hashing that directly incorporates affinity to learn binary codes. However, due to binary constraints, the optimization becomes intractable. To mitigate this challenge, different relaxation approaches have been proposed to reduce the computational load of obtaining binary codes and still attain a good solution. The problem with all existing relaxation methods is resorting to one or more additional auxiliary variables to attain high quality binary codes while relaxing the problem. The existence of auxiliary variables leads to coordinate descent approach which increases the computational complexity. We argue that introducing these variables is unnecessary. To this end, we propose a novel relaxed formulation for spectral hashing that adds no additional variables to the problem. Furthermore, instead of solving the problem in original space where number of variables is equal to the data points, we solve the problem in a much smaller space and retrieve the binary codes from this solution. This trick reduces both the memory and computational complexity at the same time. We apply two optimization techniques, namely projected gradient and optimization on manifold, to obtain the solution. Using comprehensive experiments on four public datasets, we show that the proposed efficient spectral hashing (ESH) algorithm achieves highly competitive retrieval performance compared with state of the art at low complexity.

1 Introduction

By the advance of digital technologies, we are witnessing data explosion more than before. This data carries valuable information which can help many industries, e.g., healthcare, to rely on more effective procedures. At the same time, as the size of available data gets bigger, it becomes more challenging to maintain and extract value from it. Two main issues that come with big data are the need for significant storage and computational resources. A well-known approach to address these challenges is “hashing” which refers to learning similarity preserving binary codes for data e.g., for images. Learning such representations offers two obvious advantages. First, it considerably reduces the amount of memory for saving massive data, and second, the computational efficiency that comes with calculating Hamming distances for matching. One of the most important usages of this technique is approximate nearest neighbour search

*Corresponding author

(ANN) which has many applications. Some examples are image annotation [1], large-scale clustering [2], image patch matching [3] and video segmentation [4].

Hashing algorithms can be classified into data-independent and data-dependent methods [5]. In data-independent algorithms, no information from data is used to obtain binary codes. An example is locality sensitivity hashing [6] and its extensions [7] where random projections are employed to achieve binary representations. As there is no training phase in these algorithms, their deployment is fairly easy in practice. However, this simplicity also degrades the performance of these algorithms for compact binary codes. Note that using high dimensional binary representations increases both computational and memory efficiency which goes against the initial motivations for developing hashing algorithms.

In data-dependent algorithms, either affinity information or both affinity and label information in training data are employed to transform data from Euclidean space to compact binary representation in Hamming space. The former methods are known as unsupervised hashing algorithms (which is the focus of this paper) and the latter ones are supervised hashing methods. Due to incorporating label information, supervised hashing achieves superior performance compared with unsupervised case [8, 9]. Recently, deep learning has significantly improved the state-of-art performance of hashing algorithms [8, 9]. However, there are two limitations in employing deep hashing algorithms in practice. First, they are usually supervised methods meaning that they take advantage of both label and affinity representation to obtain binary codes. Second, this significant performance comes with high computational and storage overhead. However, in practice, unsupervised hashing may be more useful as in many real-world applications the available data is unlabeled or labeling the data is prohibitively expensive. Besides, due to high number of parameters in deep hash functions their test time encoding can be slow which is against the philosophy of employing hashing.

The main issue in solving hashing problems is the discrete nature of the problem that leads to difficult optimization problems. In the iterative quantization (ITQ) algorithm [10] the authors proposed a two-step approach to compress and quantize the data. In the first step, data was projected into a rotation invariance space by applying PCA. Then, in the next step, using an alternating optimization approach the optimal rotation is found to minimize the quantization error. A similar two-step approach was employed in the isotropic hashing (Isohash) [11] where instead of minimizing quantization loss, the authors targeted to equalize the variance across different projections. The K-nearest neighbour hashing algorithm (KNNH) [12] is also a new development based on the ITQ skeleton where a heuristic approach was suggested to minimize conditional entropy of deriving binary codes. Simultaneous Compression and Quantization (SCQ) [13] is another work based on ITQ that attempts to combine dimensionality reduction and quantizations steps. Another line of research to deal with challenging optimization problems faced in learning binary representation is encoder-decoder architecture. As an example, see Binary Auto-encoder (BA) [14]. Further, an alternative for learning similarity preserving binary codes is the formulation presented in spectral hashing (SH) [15] which is based on graph Laplacian. The SH is a natural approach as it incorporates the affinity matrix directly into deriving affinity-preserving binary codes. However, the mentioned SH method has two main problems. First, calculating the pairwise affinity between data points is computationally expensive that is $O(n^2 \times d)$ where n is the number of data points and d data dimensionality. Second, even for one bit, the optimization problem in SH is equivalent to balanced graph partitioning which is a hard problem. As a result, different attempts have been made to address these limitations.

The focus of this paper is to improve the current solutions for spectral hashing formulation both in terms of training complexity and retrieval performance. Before presenting our contribution, we briefly review recent developments for spectral hashing.

To reduce the computational complexity of calculating affinity matrix, authors in hashing with graphs paper (AGH) [16] suggested employing neighborhood graph to derive a low-rank approximation of the affinity matrix. The complexity of this approximation is $O(n)$. To deal with the computational complexity of the discrete optimization faced in spectral hashing, initially, continuous relaxation was proposed. However, in this simplified approach, the binarization step destroys the learned manifold structure and degrades the quality of binary codes. To mitigate this issue, some authors proposed to incorporate a quantization loss. For example, spectral rotation (LGHSR) [17] a two-step approach similar to the idea in ITQ, was recently introduced which finds the optimal rotation that minimizes the quantization loss. In discrete graph hashing (DGH) [18] authors attempted to solve the relaxed problem and minimize the distance between continuous and the binary set simultaneously. In robust discrete hashing (RDSH) [19], an objective function for obtaining the relaxed solution along with both optimal rotation for reducing quantization loss and hash function was developed. Finally, authors of discrete spectral hashing (DSH) [20] recently proposed another approach to joint optimization over relaxed variables with minimum quantization. They showed that their solution achieves better performance while reducing training complexity.

Although different methods have been proposed to achieve better relaxed solutions while reducing complexity, we should note that all of the proposed methods including LGHSR, DGH, RDSH, and DSH employ an alternating approach

between two or more optimization variables and keep the binary decision variable in problem. We argue that this is unnecessary.

In this paper, we develop a new formulation that allows us to convert optimization problem with $n \times k$ parameters to a problem with $d \times k$ decision variables (d dimensionality and k number of bits) where $d \ll n$. Besides, in the proposed formulation the optimization problem is a function of one decision variable and as a result, the optimization is non-alternating which significantly reduces computational complexity. Two optimization algorithms are employed to obtain a solution for suggested optimization problem. The results on four public datasets show that the proposed formulation outperforms state of the art and at the same time is more efficient compared with recent algorithms proposed for graph Laplacian hashing problem.

2 Spectral Hashing

Let $\mathbf{X} \in \mathbb{R}^{n \times d}$ denote a mean zero, unit variance data matrix with rows representing training data points, each of dimensionality d . The original spectral hashing formulation [15] is as follows:

$$\begin{aligned} & \operatorname{argmin} \sum_{i,j} A_{i,j} \|\mathbf{b}_i - \mathbf{b}_j\|^2 \\ & \text{s.t. } \sum_i \mathbf{b}_i = \mathbf{0}, \quad \frac{1}{n} \sum_i \mathbf{b}_i \mathbf{b}_i^T = \mathbf{I}_k, \quad \mathbf{b}_i \in \{-1, 1\}^k \end{aligned} \quad (1)$$

where \mathbf{b}_i and \mathbf{b}_j are k -bit binary codes corresponding to the i -th and j -th data points, respectively, \mathbf{I}_k is a k by k identity matrix, and $A_{i,j}$ is the (i, j) entry of the affinity matrix \mathbf{A} , measuring the similarity between the i -th and j -th data points. Let's denote the k -bit binary representation of the data matrix \mathbf{X} by $\mathbf{B} \in \{-1, 1\}^{n \times k}$. Suppose \mathbf{D} is an $n \times n$ diagonal matrix whose diagonal element i is given by $D_{i,i} = \sum_j A_{i,j}$, then the matrix form of optimization problem can be written as

$$\begin{aligned} & \operatorname{argmin}_{\mathbf{B}} \operatorname{Tr}\{\mathbf{B}^T (\mathbf{D} - \mathbf{A}) \mathbf{B}\} \\ & \text{s.t. } \mathbf{B}^T \mathbf{B} = n \mathbf{I}_k, \quad \mathbf{B}^T \mathbf{1}_{n \times 1} = \mathbf{0}, \quad \mathbf{B} \in \{-1, 1\}^{n \times k} \end{aligned} \quad (2)$$

where Tr represents the trace operation, $\mathbf{L} = \mathbf{D} - \mathbf{A}$ is the graph Laplacian matrix [21], and $\mathbf{1}_{n \times 1}$ is a vector of length n with all elements being 1.

To reduce the computational complexity of calculating the affinity matrix \mathbf{A} from $O(n^2 d)$ to $O(n)$, we employ the low-rank approximation of [16]. This approximation is based on a small number (m) of data points, i.e. anchors, with $m \ll n$. Generally, the m cluster centers obtained from the K-means algorithm, after running a few iterations, are considered as m anchors u_j for $j = 1, \dots, m$. These anchors are used to construct an $n \times m$ affinity matrix \mathbf{Z} using Gaussian kernel of pairwise distances between the n observed data points and m anchors. In other words, the (i, j) entry of the matrix \mathbf{Z} is given by $Z_{i,j} = K(x_i, u_j) / N_0$ where x_i is the i -th data point, $K(x_i, u_j) = \exp(\|x_i - u_j\|_2^2 / \sigma^2)$, and σ is a hyperparameter. To impose sparsity on \mathbf{Z} , only distances from $s \ll m$ nearest neighbour anchors are kept and the rest are set to 0. Further, the normalization factor N_0 is calculated as $\sum_{j \in \langle i \rangle} K(x_i, u_j)$ and the normalized low-rank approximation of the affinity matrix (which is also sparse) can be calculated as $\mathbf{A} = \mathbf{Z} \mathbf{\Lambda}^{-1} \mathbf{Z}^T$ with $\mathbf{\Lambda} = \operatorname{diag}(\mathbf{Z}^T \mathbf{1})$. Finally, note that after using this low-rank approximation, we have $\mathbf{D} = \mathbf{I}$.

3 Efficient Spectral Hashing

To develop the efficient spectral hashing (ESH) algorithm, first recall that the problem in equation 2 can be written as:

$$\begin{aligned} & \operatorname{argmin}_{\mathbf{B}} -\operatorname{Tr}\{\mathbf{B}^T \mathbf{A} \mathbf{B}\} \\ & \text{s.t. } \mathbf{B}^T \mathbf{B} = n \mathbf{I}_k, \quad \mathbf{B}^T \mathbf{1}_{n \times 1} = \mathbf{0}, \quad \mathbf{B} \in \{-1, 1\}^{n \times k} \end{aligned} \quad (3)$$

As it was pointed out, even for a single bit, this problem is very difficult, and generally continuous relaxations are used to simplify the problem. However, a naive relaxation generally degrades the quality of binary codes and for this reason,

finding better continuous relaxations have been an area of research. Now, we take the first step towards efficiency. We assume the binary codes can be obtained from the following simple model:

$$\mathbf{B} = \text{sgn}(\mathbf{X}\mathbf{W}), \quad (4)$$

where \mathbf{W} is a $d \times k$ matrix and $\text{sgn}(\cdot)$ is the element-wise sign operation. Given this model, the $n \times k$ optimization variable is replaced with the $d \times k$ matrix \mathbf{W} . Clearly, $d \ll n$ so the proposed model reduces the search space. In this case, the optimization problem in Eq. 3 will turn to the following problem:

$$\begin{aligned} \underset{\mathbf{W}}{\text{argmin}} \quad & -\text{Tr}\{\text{sgn}(\mathbf{W}^T \mathbf{X}^T) \mathbf{A} \text{sgn}(\mathbf{X}\mathbf{W})\} \\ \text{s.t.} \quad & \text{sgn}(\mathbf{X}\mathbf{W})^T \text{sgn}(\mathbf{X}\mathbf{W}) = n\mathbf{I}_k, \\ & \text{sgn}(\mathbf{X}\mathbf{W})^T \mathbf{1}_{n \times 1} = \mathbf{0}. \end{aligned} \quad (5)$$

Note that after obtaining \mathbf{W} , the binary matrix \mathbf{B} can be calculated using Eq. 4. Although the mentioned model reduces the search space, due to $\text{sgn}(\cdot)$, this is still a discrete optimization problem, and difficult to solve. Removing the $\text{sgn}(\cdot)$ will result in poor binary codes due to accumulated quantization error. However, if we make sure the elements of $\mathbf{X}\mathbf{W}$ are close enough to +1 or -1, then the $\mathbf{X}\mathbf{W} \approx \text{sgn}(\mathbf{X}\mathbf{W})$ approximation is not unrealistic anymore. To make this happen, we propose a novel regularization term that pushes the elements of $\mathbf{X}\mathbf{W}$ closer to ± 1 without adding any other optimization variables. This is particularly different from methods like LGSHR, DGH, RDSH, and DSH as all of them do this by including one or more optimization variables which leads to alternating optimization approaches. Our proposed relaxed optimization problem function has the following form:

$$\begin{aligned} \underset{\mathbf{W}}{\text{argmin}} \quad & -\text{Tr}\{\mathbf{W}^T (\mathbf{X}^T \mathbf{A} \mathbf{X}) \mathbf{W}\} + \frac{\alpha}{2} \|\mathbf{X}\mathbf{W} - \mathbf{J}\|_F^2 \\ \text{s.t.} \quad & \mathbf{W}^T \mathbf{X}^T \mathbf{X} \mathbf{W} = n\mathbf{I}_k, (\mathbf{X}\mathbf{W})^T \mathbf{1}_{n \times 1} = \mathbf{0}, \end{aligned} \quad (6)$$

where \mathbf{J} is a $n \times k$ all elements equal to one matrix, $|\cdot|$ represents element-wise absolute value, and $\|\cdot\|_F$ denotes Frobenius norm. To continue, first, note that as the data is zero-centered, the last constraint in Eq. 6 is already satisfied so we remove that from the problem statement. Besides, to further simplify the problem we transform the orthogonality of columns of $\mathbf{X}\mathbf{W}$ to orthonormality of columns of \mathbf{W} . Finally, we normalize the cost function by number of samples to have a smoother training. Taking these changes into account and denoting $\mathbf{X}^T \mathbf{A} \mathbf{X}$ as \mathbf{S} which is a $d \times d$ matrix, the problem in Eq. 6 will take the following form:

$$\begin{aligned} \underset{\mathbf{W}}{\text{argmin}} \quad & \mathcal{L}(\mathbf{W}) = \frac{-1}{n} \text{Tr}\{\mathbf{W}^T \mathbf{S} \mathbf{W}\} + \frac{\alpha}{2n} \|\mathbf{X}\mathbf{W} - \mathbf{J}\|_F^2 \\ \text{s.t.} \quad & \mathbf{W}^T \mathbf{W} = \mathbf{I}_k. \end{aligned} \quad (7)$$

To solve this constraint optimization problem, two algorithms, namely projected gradient and Stiefel manifold optimization are employed.

3.1 Projected Gradient-ESH1

In this algorithm, in each iteration, the matrix \mathbf{W} is updated using the gradient descent method as if there is no constraint and then the updated matrix is projected to the closest matrix in the feasible set. The derivative of the first term in Eq. 7 is $2\mathbf{S}\mathbf{W}$. For the derivative of second part, first note that we have $|\mathbf{X}\mathbf{W}| = \text{sgn}(\mathbf{X}\mathbf{W}) \odot \mathbf{X}\mathbf{W}$ where \odot is Hadamard (element-wise) product. Then, the derivative can be calculated as follows:

$$\begin{aligned} & \frac{\partial}{\partial \mathbf{W}} \|\mathbf{X}\mathbf{W} - \mathbf{J}\|_F^2 \\ &= \frac{\partial}{\partial \mathbf{W}} \text{Tr}((|\mathbf{X}\mathbf{W}| - \mathbf{J})^T (|\mathbf{X}\mathbf{W}| - \mathbf{J})) \\ &= 2 \mathbf{X}^T \text{sgn}(\mathbf{X}\mathbf{W}) \odot (|\mathbf{X}\mathbf{W}| - \mathbf{J}) \\ &= 2 \mathbf{X}^T (\mathbf{X}\mathbf{W} - \text{sgn}(\mathbf{X}\mathbf{W})). \end{aligned} \quad (8)$$

This derivative is valid everywhere except for zero. For zero, we define the derivative equal zero. In this case if define the derivative of cost function in Eq. 8 in iteration p as \mathbf{G} then it can be calculated as follow

$$\mathbf{G}_p = \frac{-2}{n} \mathbf{S} \mathbf{W}_p + \frac{\alpha}{n} \mathbf{X}^T (\mathbf{X} \mathbf{W}_p - \text{sgn}(\mathbf{X} \mathbf{W}_p)), \quad (9)$$

In this case the learning rule for minimization the expression can be written as:

$$\mathbf{W}_p = \mathbf{W}_{p-1} - \eta \mathbf{G}_{p-1}, \quad (10)$$

where η is the learning rate parameter. To complete the iteration step, we need to project \mathbf{W} onto the feasible set. This is equivalent to finding the closest matrix \mathbf{Q} to the \mathbf{W} such that $\mathbf{Q}^T \mathbf{Q} = \mathbf{I}_k$. This problem is known as the projection on the Stiefel manifold which can be formulated as

$$\begin{aligned} \text{Proj}(\mathbf{W}) &:= \underset{\mathbf{Q}}{\text{argmin}} \quad \|\mathbf{W} - \mathbf{Q}\|_F^2 \\ \text{s.t.} \quad &\mathbf{Q}^T \mathbf{Q} = \mathbf{I}_k. \end{aligned} \quad (11)$$

Fortunately, there is a closed form solution for this problem:

$$\mathbf{Q} = \text{Proj}(\mathbf{W}) = \mathbf{U} \mathbf{I}_{d \times k} \mathbf{V}^T, \quad (12)$$

where $\mathbf{W} = \mathbf{U} \mathbf{\Sigma} \mathbf{V}^T$ is the SVD decomposition of \mathbf{W} . Interested readers can see the [22] for the detailed proof. Algorithm 1 summarizes the proposed projected gradient method.

Algorithm 1 The Proposed ESH1 Algorithm

Input: Training data $\mathbf{X} \in \mathbb{R}^{n \times d}$, affinity matrix $\mathbf{A} \in \mathbb{R}^{n \times n}$, number of iterations N , learning rate η .
Output: Binary matrix $\mathbf{B} \in \{-1, 1\}^{n \times k}$.
Initialization: Initialize an orthogonal matrix \mathbf{W} :
 $\mathbf{W}_0 \in \mathbb{R}^{d \times k}$

- 1: $\mathbf{S} \leftarrow \mathbf{X}^T \mathbf{A} \mathbf{X}$
- 2: Compute α according to Eq .19
- 3: **for** $p = 1, 2, \dots, N$ **do**
- 4: $\mathbf{W}_p \leftarrow \mathbf{W}_{p-1} - \eta \left(\frac{-2}{n} \mathbf{S} \mathbf{W}_{p-1} + \frac{\alpha}{n} \mathbf{X}^T (\mathbf{X} \mathbf{W}_{p-1} - \text{sgn}(\mathbf{X} \mathbf{W}_{p-1})) \right)$
- 5: $\mathbf{U} \mathbf{\Sigma} \mathbf{V}^T \leftarrow \text{SVD}(\mathbf{W}_p)$
- 6: $\mathbf{Q} \leftarrow \text{Proj}(\mathbf{W}) = \mathbf{U} \mathbf{I}_{d \times k} \mathbf{V}^T$
- 7: $\mathbf{W}_p \leftarrow \mathbf{Q}$
- 8: **end for**
- 9: $\mathbf{B} \leftarrow \text{sgn}(\mathbf{X} \mathbf{W})$

3.2 Stiefel Manifold Optimization-ESH2

The problem in 7 is an optimization on Stiefel manifold and methods developed for optimization on manifolds can be used to obtain a solution. In this paper we employ the method in [23] where an efficient algorithm has been proposed to preserve updated \mathbf{W} on Stiefel manifold in each iteration. Briefly, to preserve orthogonality constraint on \mathbf{W} in each iteration we define a skew-symmetric matrix \mathbf{F} in iteration $p - 1$ as $\mathbf{F}_{p-1} = \mathbf{G}_{p-1} \mathbf{W}_{p-1}^T - \mathbf{W}_{p-1} \mathbf{G}_{p-1}^T$ and denote the updated version of the \mathbf{W} as $\mathbf{Y}(\tau)$ then using a Crank-Nicolson-like scheme we have

$$\mathbf{Y}(\tau)_p = \mathbf{W}_{p-1} - \frac{\tau}{2} \mathbf{F}_{p-1} (\mathbf{W}_{p-1} + \mathbf{Y}(\tau)_p), \quad (13)$$

where τ is the step size parameter. In this case, the closed form solution for $\mathbf{Y}(\tau)$ is given as follow

$$\mathbf{Y}(\tau)_p = \left(\mathbf{I} + \frac{\tau}{2} \mathbf{F}_{p-1} \right)^{-1} \left(\mathbf{I} - \frac{\tau}{2} \mathbf{F}_{p-1} \right) \mathbf{W}_{p-1}. \quad (14)$$

Following [23] we employ the Barzilai-Borwein (BB) method to reduce the total number of iterations:

$$\tau_p = \frac{|\text{Tr}((\mathbf{M}_p)^T (\mathbf{Y}_p))|}{\text{Tr}((\mathbf{Y}_p)^T (\mathbf{Y}_p))}, \quad (15)$$

where $\mathbf{M}_p = \mathbf{W}_p - \mathbf{W}_{p-1}$, and $\mathbf{Y}_p = \nabla \mathcal{L}(\mathbf{W}_p) - \nabla \mathcal{L}(\mathbf{W}_{p-1})$, in which $\nabla \mathcal{L}(\mathbf{W}) = \mathbf{G} - \mathbf{W} \mathbf{G}^T \mathbf{W}$ is gradients of loss function in tangent planes. Algorithm 2 summarizes the proposed manifold optimization method.

Algorithm 2 The Proposed ESH2 Algorithm

Input: Training data $\mathbf{X} \in \mathbb{R}^{n \times d}$, affinity matrix $\mathbf{A} \in \mathbb{R}^{n \times n}$, number of iterations N .
Output: Binary matrix $\mathbf{B} \in \{-1, 1\}^{n \times k}$.
Initialization: Initialize an orthogonal matrix \mathbf{W} :
 $\mathbf{W}_0 \in \mathbb{R}^{d \times k}$, step size τ .

- 1: $\mathbf{S} \leftarrow \mathbf{X}^T \mathbf{A} \mathbf{X}$
- 2: Compute α according to Eq .19
- 3: **for** $p = 1, 2, \dots, N$ **do**
- 4: $\mathbf{G}_{p-1} \leftarrow \frac{-2}{n} \mathbf{S} \mathbf{W}_{p-1} + \frac{\alpha}{n} \mathbf{X}^T (\mathbf{X} \mathbf{W}_{p-1} - \text{sgn}(\mathbf{X} \mathbf{W}_{p-1}))$
- 5: $\mathbf{F}_{p-1} \leftarrow \mathbf{G}_{p-1} \mathbf{W}_{p-1}^T - \mathbf{W}_{p-1} \mathbf{G}_{p-1}^T$
- 6: $\mathbf{Y}(\tau)_p \leftarrow (\mathbf{I} + \frac{\tau}{2} \mathbf{F}_{p-1})^{-1} (\mathbf{I} - \frac{\tau}{2} \mathbf{F}_{p-1}) \mathbf{W}_{p-1}$
- 7: $\mathbf{W}_p \leftarrow \mathbf{Y}(\tau)_p$
- 8: $\tau \leftarrow \frac{|\text{Tr}((\mathbf{M}_p)^T (\mathbf{Y}_p))|}{\text{Tr}((\mathbf{Y}_p)^T (\mathbf{Y}_p))}$
- 9: **end for**
- 10: $\mathbf{B} \leftarrow \text{sgn}(\mathbf{X} \mathbf{W})$

3.3 Out of Sample: Hashing New Data

So far, we derived binary representation for training data. To obtain binary representation for a new data point \mathbf{x}^* , the same approach as in many spectral hashing methods can be used [18, 17]. More precisely, let $\mathbf{b}(\mathbf{x}^*)$ be the binarized version of \mathbf{x}^* . Then taking a similar approach as for training we can write

$$\begin{aligned} \underset{\mathbf{b}(\mathbf{x}^*)}{\text{argmin}} \quad & \sum_i^n A(\mathbf{x}_i, \mathbf{x}^*) \|\mathbf{b}_i - \mathbf{b}(\mathbf{x}^*)\|_2^2, \\ \text{s.t.} \quad & \mathbf{b}(\mathbf{x}^*) \in \{-1, 1\}^k \end{aligned} \quad (16)$$

where $A(\mathbf{x}_i, \mathbf{x}^*) = \mathbf{z}_i \Lambda^{-1} \mathbf{z}(\mathbf{x}^*)$ and \mathbf{z}_i is the i -th row of matrix \mathbf{Z} . By expanding $\|\mathbf{b}_i - \mathbf{b}(\mathbf{x}^*)\|_2^2$, it turns out this problem can be written as

$$\begin{aligned} \underset{\mathbf{b}(\mathbf{x}^*)}{\text{argmax}} \quad & \langle \mathbf{b}(\mathbf{x}^*), \mathbf{B}^T \mathbf{Z} \Lambda^{-1} \mathbf{z}(\mathbf{x}^*) \rangle, \\ \text{s.t.} \quad & \mathbf{b}(\mathbf{x}^*) \in \{-1, 1\}^k. \end{aligned} \quad (17)$$

In this case, the solution is

$$\mathbf{b}(\mathbf{x}^*) = \text{sgn}(\mathbf{B}^T \mathbf{Z} \Lambda^{-1} \mathbf{z}(\mathbf{x}^*)). \quad (18)$$

4 Experiments**4.1 Datasets and Evaluation Protocol**

The proposed ESH1 and ESH2 algorithms are validated on four benchmark datasets, namely CIFAR-10 [24], NUS-WIDE [25], LabelMe-12-50K [26], and NCT-CRC-HE-100K [27], a set of medical images.

The **CIFAR-10** contains 60,000 color images of size 32×32 pixels from 10-classes. The **NUS-WIDE** covers 269,000 images collected from Flickr. This dataset is multi-label and contains 81 ground-truth concepts. The **LabelMe-12-50K**, a highly imbalanced dataset, has 12 classes and consists of 50,000 images of size 256×256 . Images have multiple label values between zero and one. Here, following the common setting [12], the most probable class is considered as the image label. The **NCT-CRC-HE-100K** is a 9-class dataset including 100,000 non-overlapping 224×224 image patches of colorectal cancer and normal tissue.

The standard measures are employed to validate the performance of the ESH. These criteria involve *mean Average Precision* (mAP), *precision at N samples* (e.g., precision@1000), and *precision at radius 2* (precision@r=2) which calculates the precision for retrieving images with Hamming distance equal or less than 2 from the query image. If no image is found at radius 2, the precision is considered zero for that query. As LabelMe-12-50K is an imbalanced dataset, following previous works setting, the *macro average* mAP is reported to steer clear of the bias.

4.2 Implementation note

To avoid tuning parameters, we set the learning rate parameter for all datasets and experiments to a fixed value ($\eta = 0.01$). Furthermore, we propose a novel way to determine the regularization parameter α for each dataset automatically. To this end, let call the first and second terms in Eq. 7 as \mathbf{T}_1 and \mathbf{T}_2 , respectively. If we denote the initialization of \mathbf{W} as \mathbf{W}^0 , then we propose to set α such that the importance of the first and second part of the cost function is the same in the first iteration:

$$|\mathbf{T}_1(\mathbf{W}^0)| = \frac{\alpha}{2} |\mathbf{T}_2(\mathbf{W}^0)| \Rightarrow \alpha = \left| \frac{2\mathbf{T}_1(\mathbf{W}^0)}{\mathbf{T}_2(\mathbf{W}^0)} \right|. \quad (19)$$

For low-rank affinity construction, following the common setting in the graph hashing papers, we set $m = 300$ and $s = 3$ [20, 18]. The ESH code is provided in the supplementary material.

4.3 Results on LabelMe-12-50K

For this imbalanced dataset, we report macro mAP. The VGG network was employed for feature extraction. For test & train split, same as the common setting, we sample 10% of each class as test data and 90% as the training set. Table 1 represents the performance of ESH1 and ESH2 compared with other methods. It is obvious that except for 16-bit setting where DSH obtains better performance, for the 32, 64, and 128 bits ESH1 and ESH2 attain better macro mAP compared to other algorithms. In Table 1, SpH is spherical hashing [28] and KMH stands for k-means hashing [29].

Table 1: Comparison of retrieval performance, for 16, 32 and 64 bits based on macro mAP (average over classes) for LabelMe-12-50k dataset represented by 4096-D VGG-FC7 descriptor. The best performance values are highlighted in boldface.

Method	macro mAP %			
	16 Bit	32 Bit	64 Bit	128 Bit
SH	12.60	12.59	12.24	-
SpH	13.59	15.10	17.03	-
KMH	13.36	15.47	16.58	-
BA	16.96	18.42	20.80	-
ITQ	17.61	18.65	20.10	21.49
DGH	21.45	22.74	25.41	26.77
LGHSR	21.10	23.49	23.98	22.85
KNNH	20.13	23.34	26.06	27.62
DSH	24.70	23.78	24.35	22.39
SCQ	22.89	24.95	26.50	26.35
ESH1	22.95	25.67	27.59	28.94
ESH2	22.87	26.85	28.20	29.61

4.4 Results on CIFAR-10

For CIFAR-10, same as [12], each image is represented by a deep 4096-D feature extracted from VGG network [30]. For test & train split, 10% of each class is sampled as the query set and the remaining instances as the training set. Table 2 shows the results for CIFAR-10 based on mAP, precision@1000 and precision@r=2. As it can be seen, ESH1 and ESH2 outperform state of the art, namely LGHSR, KNNH, and DSH based on mAP and precision@1000 for all 16, 32, 64, and 128-bit settings. As for precision@r=2, ESH1 and ESH2 achieve the best performance for 64 and 16 bits, respectively, and competitive results for 32 bits. The first row in Fig. 1 compares the performance of the ESH algorithms with recent competitive algorithms, LGHSR, DSH, and KNNH based on precision-recall graphs. Clearly, ESH algorithms achieve better performance than recent methods.

4.5 Results on NUS-WIDE

For this multi-label dataset, the same as the common setting [16], VGG features were used for image representation. The images that their labels are among the 21 most frequent labels (195,834 images) are selected. We randomly sampled 100 images from each class to construct the test set and the rest of the images were used for training the hash function and populating the hash table. For mAP and precision calculation, two images are considered neighbours if they share at least one common label. Table 3 represents validation of ESH1 and ESH2 algorithms on this dataset. Here, LSH is

Table 2: Comparison of retrieval performance, based on mAP, precision@1000, and precision@r=2 on CIFAR-10 represented by 4096-D VGG-FC7 features. The best performance values are highlighted in boldface.

Method	mAP %				precision % @1000				precision@r=2		
	16 Bits	32 Bits	64 Bits	128 Bits	16 Bits	32 Bits	64 Bits	128 Bits	16 Bits	32 Bits	64 Bits
SH	18.31	16.54	15.78	-	-	-	-	-	-	-	-
SpH	18.82	20.93	23.40	-	-	-	-	-	-	-	-
KMH	18.68	20.82	22.87	-	-	-	-	-	-	-	-
BA	25.38	26.16	27.99	-	-	-	-	-	-	-	-
ITQ	26.23	26.73	27.90	29.22	36.71	38.79	40.75	42.53	39.33	27.71	00.06
DGH	27.73	27.44	28.01	29.47	40.36	39.46	39.70	40.69	38.73	42.25	44.04
LGSHR	27.83	25.87	22.12	19.66	39.98	42.84	41.82	40.45	38.45	46.11	32.75
KNNH	29.25	30.55	32.60	33.68	38.13	40.51	43.32	44.57	37.66	24.95	03.43
DSH	27.72	25.36	22.12	19.55	40.36	42.87	41.80	40.57	38.73	45.69	26.15
SCQ	27.52	27.42	30.34	32.25	34.24	36.51	40.29	43.15	30.58	38.24	25.14
ESH1	32.11	33.08	34.47	34.92	38.67	42.15	44.75	45.70	35.03	43.59	44.26
ESH2	31.59	33.44	34.72	35.29	41.32	43.47	45.16	45.95	38.73	46.69	43.58

Table 3: Comparison of retrieval performance based on mAP, precision@5000, and precision@r=2 on NUS-WIDE dataset represented by VGG-F deep features. The best performance values are highlighted in boldface.

Method	mAP %				precision % @5000				precision@r=2		
	16 Bits	32 Bits	64 Bits	128 Bits	16 Bits	32 Bits	64 Bits	128 Bits	16 Bits	32 Bits	64 Bits
LSH	40.45	48.04	46.75	-	47.95	55.29	58.95	-	-	-	-
SH	44.74	42.60	42.36	-	59.15	54.98	54.18	-	-	-	-
AGH	49.80	47.14	44.72	-	70.43	70.29	69.29	-	-	-	-
SGH	48.86	49.10	51.33	-	64.92	66.04	69.01	-	-	-	-
ITQ	52.09	53.12	54.04	54.85	64.34	66.62	68.48	69.54	67.31	51.91	05.21
DGH	51.35	52.21	53.34	55.96	66.33	65.35	66.02	67.20	65.14	68.41	70.19
LGHSR	50.06	47.72	45.71	44.11	68.42	68.09	67.92	66.95	68.87	71.98	45.27
KNNH	55.12	57.03	58.61	59.45	66.77	69.83	71.07	72.13	68.61	49.78	09.58
DSH	49.87	47.07	45.67	44.03	68.05	68.17	67.83	67.15	68.67	71.86	39.93
SCQ	56.34	56.21	56.10	53.54	68.45	70.64	70.81	69.00	68.74	70.92	08.98
ESH1	56.32	56.89	57.47	57.28	67.58	69.47	71.46	72.31	64.64	72.30	60.14
ESH2	56.54	57.16	57.71	57.53	68.20	70.80	72.14	72.45	64.34	72.06	62.08

locality sensitivity hashing [31], PCAH is semi-supervised hashing [32], and SGH represents salable graph hashing [33]. For mAP, ESH1 and ESH2 are outperforming DSH the most recent method based on spectral hashing formulation. Besides, the results are highly competitive with the state of the art method KNNH. Note that in the KNNH method there exists an $O(n^2d)$ complexity for distances computing and a $O(n^2 \log_2 n)$ complexity for sorting while ESH1 method is by far more efficient with a complexity of $O(2ndkN + ndm)$. Based on precision@5000 for all bit settings, the ESH2 method achieves the best result. Besides, this is clear from precision-recall graphs in the second row of Fig. 1, the ESH algorithms are competitive compared with the state of the art.

4.6 Results on NCT-CRC-HE-100K

For NCT-CRC-HE-100K dataset, EfficientNet [34] pre-trained on ImageNet was used for feature extraction. The training set consists of 70,000 randomly sampled images and the test set includes the remaining 30,000 images. Table 4 illustrates that ESH1 and ESH2 are achieving the best performance in terms of mAP for 16, 32, 64, and 128 bits. For the precision@1000, DSH achieves the best result and ESH2 achieves 2% less precision. However, as the number of bits increases, the performance of the ESH algorithms increases with a stronger trend such that for 32-bit setting ESH2 and DSH perform equally and ESH algorithms outperform DSH for 64 and 128 bits with a margin of 3% and 5%, respectively. Clearly, ESH algorithms attain the best performance for precision@r=2 in the 64-bit setting. Although for 16 and 32-bit settings, DSH and LGHSR reach the best performance, the ESH algorithms are still competitive. The third row in Fig. 1, illustrates how the ESH algorithms are performing compared with recent methods in terms of precision-recall graphs. Almost in all cases, the ESH algorithms are achieving better performance compared with other methods.

Table 4: Comparison of retrieval performance based on mAP, precision@1000, and precision@r=2 on NCT-CRC-HE-100K dataset represented by EfficientNet features. The best performance values are highlighted in boldface.

Method	mAP %				precision % @1000				precision@r=2		
	16 Bits	32 Bits	64 Bits	128 Bits	16 Bits	32 Bits	64 Bits	128 Bits	128 Bits	32 Bits	64 Bits
ITQ	54.72	55.78	57.50	58.39	68.41	71.64	74.63	76.14	67.90	72.54	35.66
DGH	49.85	47.24	51.61	59.61	74.08	77.14	77.05	77.58	68.75	79.02	79.15
LGHSR	55.28	47.74	38.65	32.37	75.66	78.21	77.13	74.67	73.80	79.82	67.76
KNNH	58.02	61.47	64.28	65.79	70.27	74.91	78.16	80.30	68.37	69.56	42.73
DSH	58.75	45.63	37.27	32.52	76.70	78.71	77.73	75.30	75.15	79.56	61.49
SCQ	64.90	67.25	67.75	66.57	76.03	80.07	80.01	80.02	69.64	80.51	72.65
ESH1	66.32	66.77	67.14	66.26	74.82	77.36	79.84	80.32	67.14	76.92	80.02
ESH2	63.54	67.30	67.75	67.04	71.85	78.12	80.16	80.46	63.04	77.17	80.41

4.7 Effect of Regularization

To see how incorporating the introduced regularization term in Eq .7 improves the quality of binary codes, we ran experiments with $\alpha = 0$ on NCT-CRC-HE-100K. Table 5 shows setting $\alpha = 0$ significantly degrades the performance confirming the effectiveness of the proposed regularization.

Table 5: Effect of the regularization term on retrieval performance in terms of mAP for NCT-CRC-HE-100K dataset.

Method, Regularization	NCT-CRC-HE-100K			
	16 Bit	32 Bit	64 Bit	128 Bit
ESH1, $\alpha = 0$	40.65	35.96	31.09	26.80
ESH1, $\alpha=\text{automatic}$	66.32	66.77	67.14	66.26

4.8 Model Complexity

In this section, we provide a complexity analysis of the ESH1 algorithm and compare it with recent representative graph hashing methods. The complexity for calculating matrix \mathbf{S} which only needs to be calculated once is $O(ndm)$. Besides, for the learning rule in the projected gradient method, the complexity is $O(2ndkN)$ and as a result, the overall complexity is $O(2ndkN + ndm)$. Table 6 presents the complexity of the proposed ESH1 algorithm and recent representative graph hashing methods without including affinity matrix complexity. Clearly, the RDSH algorithm has the highest time complexity $O(n^3)$ which is due to solving a standard Sylvester equation for deriving spectral solution. On the other hand, the AGH algorithm has the lowest complexity as it uses eigen decomposition for obtaining spectral solution. As for other algorithms in Table 6, they are a function of at least two decision variables that increase the complexity. For example, the term $nkN \log_2 n$ in LGHSR and DSH represents the complexity for updating additional variable non-existent in ESH algorithms. On the other hand, ESH has lower complexity as the optimization is function of one variable, and there is no inner loop, e.g., terms like $N_G N$ in DSH or $N_B N$ in DGH in iterations.

Table 6: Comparison of time complexities.

Method	Time complexity
AGH	$O(m^2n + (s + 1)kn)$
DGH	$O(nmkN_B N + k^2nN)$
RDSH	$O(n^3)$
LGHSR	$O(m^2n + (s + 1)kn + 2nk^2N + nkN \log_2 n)$
DSH	$O(nmkN_G N + nkN \log_2 n)$
ESH	$O(2ndkN + ndm)$

4.9 Comparison with deep unsupervised hashing

Although deep learning mainly has been applied to supervised hashing problem, recently some attempts have been made to develop deep unsupervised hashing methods. Some examples include DH [35], UHBDNN [36], DeepBit [37], and SADH [38]. Table 7 compares performance of our proposed method compared with these algorithms. Clearly,

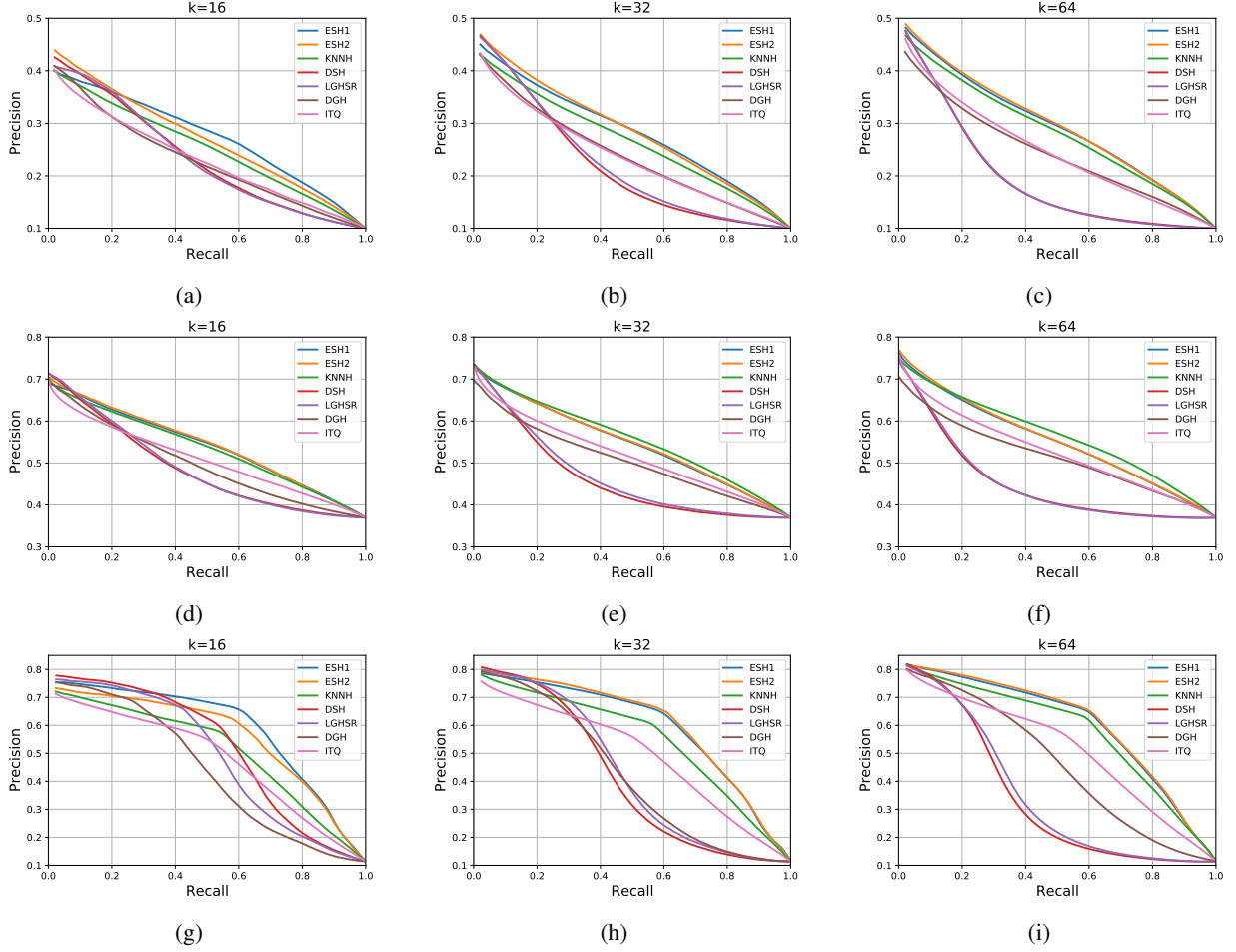


Figure 1: Precision-recall graphs for CIFAR-10 (first row), NUS-WIDE (second row), and NCT-CRC-HE-100K (third row) for different number of bits ($k = 16, 32, 64$).

based on Table 7 ESH 1 and ESH 2 outperform UHBDNN and DeepBit and provide competitive results compared with SADH. In this Table, “R+” imply that raw images are fed to the network suggesting that these methods are end to end. On the other hand, “V+” means vector representations are fed to the network. Considering the simplicity of our proposed method compared with deep methods the feature learning has not been included the obtained results are promising.

Table 7: ESH compared with deep unsupervised hashing algorithms for NUS-WIDE dataset. The R+ and V+ means the respective algorithm works on raw images and vector data (images after feature extraction) respectively.

Method	mAP %			precision % @5000		
	16 B	32 B	64 B	16 B	32 B	64 B
V+UHBDN	54.26	51.72	54.74	70.18	69.60	72.74
R+DeepBit	39.22	40.32	42.06	45.54	51.34	57.72
R+SADH	60.14	57.99	56.33	71.45	73.88	75.04
ESH1	56.32	56.89	57.47	67.58	69.47	71.46
ESH2	56.54	57.16	57.71	69.74	72.49	75.62

5 Conclusions

In this paper, we proposed a novel formulation for spectral hashing which achieves highly competitive performance compared with most recent methods and at the same time, enjoys low complexity. The proposed projected gradient

method is highly efficient for three reasons. Firstly, the formulation for ESH transforms the decision variable with dimensionality of $n \times k$ to $d \times k$ where $d \ll n$. Secondly, the affinity matrix which is $n \times n$ in the spectral formulation has been removed, and instead, a $d \times d$ matrix \mathbf{S} plays a similar role. Finally, and more importantly, unlike other graph hashing schemes, the proposed formulation achieves high quality binary codes without adding any additional decision variables to the problem. We applied two different optimization techniques i.e., projected gradient and manifold optimization to obtain a solution. Using extensive experiments on four public datasets, we showed that the proposed method either outperforms or achieves highly competitive results compared with recent methods and offering low complexity at the same time.

References

- [1] Qifan Wang, Bin Shen, Shumiao Wang, Liang Li, and Luo Si. Binary codes embedding for fast image tagging with incomplete labels. In *European Conference on Computer Vision*, pages 425–439. Springer, 2014.
- [2] Yunchao Gong, M. Pawlowski, Fei Yang, L. Brandy, L. Boundev, and R. Fergus. Web scale photo hash clustering on a single machine. In *2015 IEEE Conference on Computer Vision and Pattern Recognition*, pages 19–27, 2015.
- [3] Simon Korman and Shai Avidan. Coherency sensitive hashing. *IEEE transactions on pattern analysis and machine intelligence*, 38(6):1099–1112, 2015.
- [4] Xiao Liu, Dacheng Tao, Mingli Song, Ying Ruan, Chun Chen, and Jiajun Bu. Weakly supervised multiclass video segmentation. In *The IEEE Conference on Computer Vision and Pattern Recognition (CVPR)*, June 2014.
- [5] Jingdong Wang, Ting Zhang, Nicu Sebe, Heng Tao Shen, et al. A survey on learning to hash. *IEEE transactions on pattern analysis and machine intelligence*, 40(4):769–790, 2017.
- [6] A. Andoni and P. Indyk. Near-optimal hashing algorithms for approximate nearest neighbor in high dimensions. In *2006 47th Annual IEEE Symposium on Foundations of Computer Science (FOCS’06)*, pages 459–468, Oct 2006.
- [7] Brian Kulis and Kristen Grauman. Kernelized locality-sensitive hashing for scalable image search. In *IEEE 12th international conference on computer vision*, pages 2130–2137, 2009.
- [8] Sepehr Eghbali and Ladan Tahvildari. Deep spherical quantization for image search. In *The IEEE Conference on Computer Vision and Pattern Recognition (CVPR)*, June 2019.
- [9] Fatih Cakir, Kun He, Sarah Adel Bargal, and Stan Sclaroff. Mihash: Online hashing with mutual information. In *Proceedings of the IEEE International Conference on Computer Vision*, pages 437–445, 2017.
- [10] Yunchao Gong, Svetlana Lazebnik, Albert Gordo, and Florent Perronnin. Iterative quantization: A procrustean approach to learning binary codes for large-scale image retrieval. *IEEE transactions on pattern analysis and machine intelligence*, 35(12), 2012.
- [11] Weihao Kong and Wu-Jun Li. Isotropic hashing. In *Advances in neural information processing systems*, pages 1646–1654, 2012.
- [12] Xiangyu He, Peisong Wang, and Jian Cheng. K-nearest neighbors hashing. In *The IEEE Conference on Computer Vision and Pattern Recognition (CVPR)*, June 2019.
- [13] Tuan Hoang, Thanh-Toan Do, Huu Le, Dang-Khoa Le-Tan, and Ngai-Man Cheung. Simultaneous compression and quantization: A joint approach for efficient unsupervised hashing. *Computer Vision and Image Understanding*, 191:102852, 2020.
- [14] M. Á. Carreira-Perpiñán and R. Raziperchikolaei. Hashing with binary autoencoders. In *2015 IEEE Conference on Computer Vision and Pattern Recognition (CVPR)*, pages 557–566, 2015.
- [15] Yair Weiss, Antonio Torralba, and Rob Fergus. Spectral hashing. In *Advances in neural information processing systems*, pages 1753–1760, 2009.
- [16] Wei Liu, Jun Wang, Sanjiv Kumar, and Shih-Fu Chang. Hashing with graphs. In *ICML*, 2011.
- [17] Xuelong Li, Di Hu, and Feiping Nie. Large graph hashing with spectral rotation. In *Proceedings of the Thirty-First AAAI Conference on Artificial Intelligence*, pages 2203–2209, 2017.
- [18] Wei Liu, Cun Mu, Sanjiv Kumar, and Shih-Fu Chang. Discrete graph hashing. In *Advances in neural information processing systems*, pages 3419–3427, 2014.
- [19] Yang Yang, Fumin Shen, Heng Tao Shen, Hanxi Li, and Xuelong Li. Robust discrete spectral hashing for large-scale image semantic indexing. *IEEE Transactions on Big Data*, 1(4):162–171, 2015.

- [20] Di Hu, Feiping Nie, and Xuelong Li. Discrete spectral hashing for efficient similarity retrieval. *IEEE Transactions on Image Processing*, 28(3):1080–1091, 2018.
- [21] Wei Liu, Junfeng He, and Shih-Fu Chang. Large graph construction for scalable semi-supervised learning. In *ICML*, 2010.
- [22] Jonathan H Manton. Optimization algorithms exploiting unitary constraints. *IEEE Transactions on Signal Processing*, 50(3):635–650, 2002.
- [23] Zaiwen Wen and Wotao Yin. A feasible method for optimization with orthogonality constraints. *Mathematical Programming*, 142(1-2):397–434, 2013.
- [24] Alex Krizhevsky, Geoffrey Hinton, et al. Learning multiple layers of features from tiny images. 2009.
- [25] Tat-Seng Chua, Jinhui Tang, Richang Hong, Haojie Li, Zhiping Luo, and Yantao Zheng. Nus-wide: a real-world web image database from national university of singapore. In *ACM international conference on image and video retrieval*, pages 1–9, 2009.
- [26] Rafael Uetz and Sven Behnke. Large-scale object recognition with cuda-accelerated hierarchical neural networks. In *2009 IEEE international conference on intelligent computing and intelligent systems*, volume 1, pages 536–541. IEEE, 2009.
- [27] Marc Macenko, Marc Niethammer, James S Marron, David Borland, John T Woosley, Xiaojun Guan, Charles Schmitt, and Nancy E Thomas. A method for normalizing histology slides for quantitative analysis. In *2009 IEEE International Symposium on Biomedical Imaging: From Nano to Macro*, pages 1107–1110. IEEE, 2009.
- [28] Jae-Pil Heo, Youngwoon Lee, Junfeng He, Shih-Fu Chang, and Sung-Eui Yoon. Spherical hashing. In *2012 IEEE Conference on Computer Vision and Pattern Recognition*, pages 2957–2964. IEEE, 2012.
- [29] Kaiming He, Fang Wen, and Jian Sun. K-means hashing: An affinity-preserving quantization method for learning binary compact codes. In *Proceedings of the IEEE conference on computer vision and pattern recognition*, pages 2938–2945, 2013.
- [30] Karen Simonyan and Andrew Zisserman. Very deep convolutional networks for large-scale image recognition. *arXiv preprint arXiv:1409.1556*, 2014.
- [31] Aristides Gionis, Piotr Indyk, Rajeev Motwani, et al. Similarity search in high dimensions via hashing. In *Vldb*, volume 99, pages 518–529, 1999.
- [32] Jun Wang, Sanjiv Kumar, and Shih-Fu Chang. Semi-supervised hashing for large-scale search. *IEEE transactions on pattern analysis and machine intelligence*, 34(12):2393–2406, 2012.
- [33] Qing-Yuan Jiang and Wu-Jun Li. Scalable graph hashing with feature transformation. In *Twenty-Fourth International Joint Conference on Artificial Intelligence*, 2015.
- [34] Mingxing Tan and Quoc V Le. Efficientnet: Rethinking model scaling for convolutional neural networks. *arXiv preprint arXiv:1905.11946*, 2019.
- [35] Venice Erin Liong, Jiwen Lu, Gang Wang, Pierre Moulin, and Jie Zhou. Deep hashing for compact binary codes learning. In *Proceedings of the IEEE conference on computer vision and pattern recognition*, pages 2475–2483, 2015.
- [36] Thanh-Toan Do, Anh-Dzung Doan, and Ngai-Man Cheung. Learning to hash with binary deep neural network. In *European Conference on Computer Vision*, pages 219–234. Springer, 2016.
- [37] Kevin Lin, Jiwen Lu, Chu-Song Chen, and Jie Zhou. Learning compact binary descriptors with unsupervised deep neural networks. In *Proceedings of the IEEE Conference on Computer Vision and Pattern Recognition*, pages 1183–1192, 2016.
- [38] Fumin Shen, Yan Xu, Li Liu, Yang Yang, Zi Huang, and Heng Tao Shen. Unsupervised deep hashing with similarity-adaptive and discrete optimization. *IEEE transactions on pattern analysis and machine intelligence*, 40(12):3034–3044, 2018.